Pulse switching in nonlinear fiber directional couplers

I. M. Uzunov,* R. Muschall, M. Gölles, Yuri S. Kivshar,† B. A. Malomed,‡ and F. Lederer
Faculty of Physics and Astronomy, Friedrich-Schiller-Universität Jena, Max-Wien-Platz 1, D-07743 Jena, Germany
(Received 1 August 1994)

A comprehensive analysis of the propagation of short pulses in fiber nonlinear directional couplers is presented. In particular, the limitations as well as the merits of the variational approach to describe power- and phase-controlled pulse switching are discussed. Relying on beam propagation calculations a trial function that accounts for variable width, amplitude, phase, and chirp of the pulses is proposed. The corresponding Euler-Lagrangian equations for the pulse parameters are derived and solved. Concerning power-controlled switching an excellent agreement of the switching curve with beam propagation results is found. Moreover, even the evolution of the various pulse parameters is shown to be described reasonably by the analytical model used. Eventually, optimum criteria for efficient phase-controlled switching may be easily derived by using the model presented.

PACS number(s): 42.81.Dp

I. INTRODUCTION

Nonlinear coherent couplers, originally invented in 1982 [1,2], have attracted a great deal of interest as basic all-optical elements because the output may be routed between the two channels as a function of the input power launched into one channel (power-controlled switching) [3,4] or the phase difference between a strong and a weak input signal in different input channels (phase-controlled switching) [5]. The stationary response of that device has been discussed in detail for numerous situations (for a summary, see, e.g., the review papers [3,4], the references therein and [5]). For the particular case when the nonlinear coherent coupler has a preferred direction of switching and the interaction between the channels is constant, it is called the nonlinear directional coupler (NLDC).

Mathematically, the problem is described in terms of a coupled mode theory (CMT) by a set of (coupled) nonlinear ordinary differential equations (ODE's) for the slowly varying amplitudes of the guided modes in both channels. That approach also holds in the nonstationary regime, provided that the pulses are sufficiently long or the waveguides are short. In that case the dispersion of the group velocity (GVD) may be neglected and, consequently, all frequency components of the pulse have a common group velocity. The time in the reference frame of the pulse enters the coupled mode equations merely as a parameter. This has the consequence that the coupling behavior (efficiency and coupling length) depends on the instantaneous intensity of the pulse at a certain time. It is evident that this leads to the detrimental pulse break up [6–12] and thus to an incomplete switching between both channels. This phenomenon limits considerably the opportunity of different cascading switching elements.

In view of this phenomenon, optical fibers have attracted a particular interest as waveguiding channels of a nonlinear directional coupler. Fused-silica optical fibers have two properties that are rarely encountered in nonlinear materials; their GVD is anomalous for wavelength $\lambda > 1.3\ \mu$m, and they exhibit an instantaneous, local, and focusing Kerr nonlinearity in that wavelength domain. Both peculiarities allow for the formation of stable, robust pulses that maintain their shape in the course of propagation even in the presence of small perturbations. Those pulses are called (bright) optical solitons, and have been at the center of both theoretical and experimental research for more than a decade [13,14]. The underlying mechanism of soliton formation can be easily understood if one looks at the interplay between the frequency chirp and the width of a short pulse. In a linear medium with nonvanishing GVD the pulse acquires a negative frequency chirp (down-chirp) in the course of propagation that leads ultimately to a pulse broadening, because the individual components of the pulse propagate with different group velocities. If an instantaneous local, focusing nonlinearity comes into the play, an additional intensity-dependent positive chirp (up-chirp) is provided by self-phase modulation that depends critically on the pulse shape. If the GVD is anomalous (this is the case we are interested in here) both contributions to the chirp may balance, provided that a certain relation among pulse width, GVD, and optical intensity holds and that the pulse has a particular shape. Because in that case the net chirp acquired vanishes, the pulse width remains constant in the course of propagation in a medium with an anomalous GVD. The exact balance appears if the pulses

*Permanent address: Institute of Electronics, Bulgarian Academy of Science, boul.Tsarigradsko shosse 72, 1784 Sofia, Bulgaria.

†Permanent address: Optical Science Center, Australian National University, Australian Capital Territory, 0200 Canberra, Australia.

‡Permanent address: Department of Applied Mathematics, School of Mathematical Sciences, Tel Aviv University, 69978 Ramat Aviv, Israel.

have the famous sech shape, although it has been shown that the behavior may be somewhat similar for Gaussian pulses with a certain relation between width and amplitude [15,16]. Keeping the remarkable robustness of solitons in mind, it may be anticipated that they prevail against the perturbation provided by the linear coupling of the guided modes taking place in the NLDC. Indeed, it has been shown numerically as well as experimentally that the detrimental pulse breakup can be avoided [17–21].

Mathematically, under approximations reasonable for picosecond pulses the evolution of the slowly varying envelope of a guided mode in an isolated, monomode fiber is governed by the nonlinear Schrödinger equation (NLSE) (see [13,14]). This equation is exactly integrable in the framework of the approach given by the inverse scattering transform (IST), leading to fundamental and higher-order solitons [22]. In a two-core NLDC the pulse dynamics may be described by two coupled NLSE's, where the coupling is coherently mediated by a linear coupling term. In contrast to the situation known as Manakov's system [23], the coupled NLSE model is not integrable. There are two opportunities left to solve the coupled system of partial differential equations (PDE's); by fully numerical or by approximate methods. Usually, one scales the system appropriately so that only one parameter is left, say the scaled coupling coefficient. This means that one may cover different physical situations in solving the system once, making numerical methods less time consuming. On the other hand, the completely numerical solution, e.g., by the beam propagation method (BPM) (see, e.g., [24] to cite a few), is not very appealing from the theoretical point of view, but it is considered to yield quite accurate results with respect to the evolution of the pulses in both channels as well as to the switching curve, and hence the critical power. That is why this method may serve as a solid benchmark in estimating the results provided by quasianalytical, and hence sometimes approximate, models. Nevertheless, it is interesting to disclose the performance of approximate models because they may become attractive if one encounters more complicated situations such as nonlinear N-core couplers that are interesting with respect both to steeper switching curves [25,26] and to their combined nature as mixed continuous-discrete systems [27,28]. Even for the two-core coupler it may turn out to be difficult to identify the critical points for phase-controlled switching if one uses purely numerical methods. Among the approximate models two are particularly popular, relying either in the constants of motion of an integrable system or on a variational approach. The idea of the former model is to rewrite the system as an integrable one (e.g., the Manakov system [23]), leaving the additional terms as perturbations [3,28–30]. The solutions of the unperturbed system are then used as trial functions with pulse parameters that are allowed to vary adiabatically with the propagation distance. Those trial functions are inserted into the conserved quantities that vary now adiabatically. Eventually, one obtains a system of effective ODE's which describes the evolution of the pulse parameters.

The variational approach was successfully applied to optical solitons by Anderson and co-workers [15,16]. Here the idea consists of using the Lagrangian for the complete system under consideration. The solutions of the decoupled system (e.g., the fundamental soliton) are then inserted into that Lagrangian where the pulse parameters may again depend on the propagation distance. A subsequent integration with respect to time leads to an averaged Lagrangian. If one performs the variations with respect to the free parameters, one ends up with the Euler-Lagrangian equations being a set of coupled ODE's. Generally, this set may be cast in a Hamiltonian form where the conjugated variables provide a clear physical picture (e.g., it turns out that phase and intensity difference in both channels as well as pulse width and chirp are conjugated variables, which agrees well with the fundamental physics of soliton formation). It is evident that both approaches are similar. The key point of both models consists of choosing appropriate trial functions, in particular in fixing the number of free parameters. Furthermore, one should be aware that both methods are integral ones, leading to the conclusion that integrated quantities (such as the energy transmission) should be predictable more precisely than the details of the evolving pulses (such as the pulse width and peak power transmission). There is another restriction that concerns the very pulse shape, that was pointed out recently [31–33]. There the authors focused their attention on stationary coupled soliton states propagating in a NLDC. It has been shown, partly analytically and partly numerically, that there are symmetric as well as antisymmetric states the wave-number shift of which depends nonlinearily on the guided intensity (nonlinear dispersion relation). Moreover, bifurcation from both solutions forming different asymmetric states could be identified. Note, however, that the asymmetric state and the bifurcation leading to it from the symmetric one was first found in Refs. [34,41] in the framework of the variational approximation. In investigating the stability of all branches of the nonlinear dispersion curve, it has been shown that the symmetric state loses stability beyond the bifurcation point, whereas the merging asymmetric state is stable. Concerning the antisymmetric state the situation appears more involved. There, numerical calculations have shown that beyond a certain energy, well below the bifurcation energy, the solution becomes unstable. This holds likewise for the complete asymmetric curve branching off from the antisymmetric one [33]. Furthermore, the authors show that soliton states may emerge, the shape of which may be different from those of the fundamental solitons. In those situations, where the pulse form seriously deviates from the trial function chosen, both approximate methods certainly fail. This may appear if one launches strong pulses into both channels of the coupler, but is not anticipated to happen if only one channel of the coupler is excited (power-controlled switching) or an additional weak signal is launched into the second channel (phase-controlled switching), as it is normally the case in a switching experiment. Here we are exclusively interested in that situation. Although the normal mode analysis [31–33] is very

interesting from the theoretical point of view, it describes only the evolution of a coupled stationary state where the power is launched initially into both cores of the guide as close as possible to a certain stationary solution. The method is not able to describe the typical situation one is interested in when inspecting switching processes; that is, when a nonstationary (with respect to the direction of propagation) state is initially excited. One can only predict that the critical power for switching is well beyond the bifurcation point.

The variational approach was applied to the coupler geometry by Paré and Florjanczyk [34]. As emphasized the crucial point of that approach consists of choosing appropriate trial functions. Obviously, the more free parameters one selects the better the results meet the exact solution. There will be a tradeoff between simplicity and exactness. Paré and Florjanczyk [34] have shown that variable amplitudes and phases, but constant widths and zero chirps, lead to an analytical solution that differs from the cw result only by a different definition of the modulus of the Jacobian elliptic function describing the coupler transmission. Consequently, the analytically predicted critical power differs from the cw case, but also by approximately 12% from the numerical result.

The most important complete trial function was proposed by Cagliotti *et al.* [35] using a momentum expansion that results in a bulky set of ODE's. Moreover, in general, the integration can be carried out only for Gaussian pulses rather than for sechlike ones. Although this model contains the other ones as particular cases, it provides no immediate insight into the switching dynamics.

Very recently, compromises between those two approaches were presented [36,37]. Kivshar [36] reduced the number of free parameters by relating the amplitudes and widths, and set the chirp to zero as it appears for isolated solitons. Obviously, this ansatz is at first glance very appealing. However, it assumes that solitons maintain their very identity at all times during the coupling process, as could be anticipated for very weak linear coupling. Furthermore, it requires an input in both channels, as it would result in an infinite width of the soliton in the initially unexcited channel for the one channel input [37], which is of particular interest for switching applications. Hence that ansatz may not be used for this situation. Alternatively, it was shown [37] that a variable but common width and zero chirp leads again to a one-degree-of-freedom model, where a particlelike picture can be adopted, and a slight improvement with respect to the results of [34] could be obtained. However, there is a fundamental objection against that approach, namely that the width and chirp are conjugated variables in the framework of a variational approach, as pointed out by Anderson and co-workers [15,16], and thus the evolution of the chirp due to linear coupling must not be neglected. A chirped trial function for an incoherently coupled system of NLSE's (orthogonal modes in birefringent fibers) with variable widths and chirps for both pulses was used in [38,39]. Furthermore, the importance of incorporating variable width and chirp was pointed out in [40]. In two recent papers [41,42] that dealt with the pulse dynamics of NLDC's, a trial function, originally proposed by Muraki and Kath [39], with variable but common width and chirp and variable but different amplitudes and phases was used. However, in the subsequent analysis the chirp was omitted and, accordingly, the widths are postulated to remain constant. Therefore, the analytical results obtained for the switching problem in [41,42] were, in fact identical to those reported by Paré and Florjanczyk [34].

The aim of the present paper is to disclose both the merits and limits of the variational approach in describing power- and phase-controlled switching in nonlinear fiber directional couplers. Furthermore, we discuss the reliability of the trial functions used.

The paper is structured as follows.

In Sec. II we briefly discuss the main results of continuous-wave (cw) switching, basically to show that the problem of the fixed pulse width may be simply mapped into it, provided a simple rescaling is made.

In Sec. III the basic equations describing the pulse switching are introduced, and physically reasonable trial functions are identified in studying numerically the evolution of the pulses along the coupler. It turns out that the shape of the pulses (sechlike) is well preserved, at least if the propagation distance does not exceed the half-beat length considerably, whereas both pulses acquire a negative chirp due to the linear coupling of both channels. Regardless of the different amplitudes, this chirp leads ultimately to a pulse spreading (increasing width) in both channels. On the basis of these findings we introduce appropriate trial functions in order to apply the variational approach in Sec. IV. We end up with the ODE's of a two-degree-of-freedom model. In Sec. V we solve those equations for the case of power-controlled switching, and compare the results obtained with those provided by BPM calculations. An excellent agreement of both approaches can be identified. Eventually, in Sec. VI we show that the optimum criteria for phase-controlled switching can be derived easily by using the variational approach. Finally Sec. VII concludes the paper.

II. MODEL AND CONTINUOUS-WAVE SWITCHING

If we assume a Kerr nonlinearity ($n=n_L+n_2I$, where I is the local intensity) in the fibers and neglect attenuation and higher-order dispersion, the coupling process is known to be described by the coupled NLSE's in standard units

$$i\frac{\partial u_\nu}{\partial \xi}+\frac{1}{2}\frac{\partial^2 u_\nu}{\partial \tau^2}+|u_\nu|^2u_\nu+Ku_{3-\nu}=0, \quad \nu=1,2 \ . \tag{1}$$

Here $\xi=z/L_D$ and $\tau=t/\tau_0$ are the normalized length and time in the reference frame of the pulse, respectively, where τ_0 is the pulse length. If β_2 is the group-velocity dispersion ($\beta_2<0$, because we are restricting to the anomalous dispersion region), A_{eff} the effective core area, n_2 the nonlinear coefficient, ω_0 the mean frequency, L_H the linear half-beat length, and A_ν the slowly varying envelope of the pulses, respectively, the normalizations read

$$L_D=\frac{\tau_0^2}{|\beta_2|},\quad \gamma=\frac{n_2\omega_0}{A_{\text{eff}}},$$
$$u_\nu=\left[\frac{\gamma\tau_0^2}{|\beta_2|}\right]^{1/2}A_\nu,\quad K=\frac{\pi}{2}\frac{L_D}{L_H}. \tag{2}$$

For convenience, in our numerical calculations we choose $k=1$ for the normalized coupling parameter. Hence the linear half-beat length equals the soliton period and is $\xi=\pi/2$. First we briefly consider the case of the cw switching, and compare it below with the results obtained for the pulse switching. In fact, the case of the cw switching is very simple because of its integrability [1]. It is described by the same system (1), but when time derivatives are assumed to be zero (no dispersion effect). In that particular case we have a system of two coupled ordinary differential equations:

$$i\frac{du_1}{d\xi}+|u_1|^2u_1=-Ku_2, \tag{3}$$

$$i\frac{du_2}{d\xi}+|u_2|^2u_2=-Ku_1. \tag{4}$$

Equations (3) and (4) conserve the total energy of the system given by the relation $I=|u_1|^2+|u_2|^2$, so that it is convenient to reduce the number of the dynamical variables introducing the additional ones

$$u_1=\sqrt{I}\cos\theta e^{i\phi_1},\quad u_2=\sqrt{I}\sin\theta e^{i\phi_2}. \tag{5}$$

The resulting system of three coupled equations can be simplified further by introducing the relative phase $\phi=\phi_1-\phi_2$, so that the final system of two dynamical equations becomes

$$\sin(2\phi)\frac{df}{d\xi}=\cos(2\theta)[-I\sin(2\theta)+2K\cos\phi], \tag{6}$$

$$\frac{d\theta}{d\xi}=K\sin\phi. \tag{7}$$

As a matter of fact, the dynamical model (6) and (7) is another form of the equations derived by Jensen [1]. However, we would like to note that in their present form Eqs. (6) and (7) are more conveniently compared with the corresponding model of soliton switching.

Equations (6) and (7) are easily integrated because they have the integral of motion (Hamiltonian)

$$H=-K\sin(2\theta)\cos\phi-\tfrac{1}{4}I\sin^2(2\theta), \tag{8}$$

and different types of dynamical regimes are described by elliptic functions [1]. However, to understand qualitatively the origin of the various types of system dynamics, the best way is to use the phase plane (θ,ϕ). Equations (6) and (7) are doubly periodic, so that the phase plane is doubly periodic too. A straightforward analysis shows that the phase plane of the dynamical system (6) and (7) displays different modifications depending on the dimensionless parameter $\alpha=I/K$. For small values of α, i.e., when $\alpha<2$, there are two sets of stable fixed points at $\phi=0$ and π which correspond to the stationary states with equal intensities of the two modes but with the same or opposite phases.

When the value of the dimensionless parameter α increases, the fixed points of the phase plane (θ,ϕ) change, and, in fact, at $\alpha=2$ the bifurcation of fixed points occurs at $\phi=0$. Therefore, the cw switching analyzed from the viewpoint of the stationary states on the phase plane (θ,ϕ) displays the critical value of the key parameters $\alpha=I/K$ when the break of stability of the trivial stationary state occurs. For $\alpha>2$ the intensity of the stationary states of two coupled modes are given by the relation

$$|u_1|^2,|u_2|^2=\frac{I}{2}\left[1\pm\left[1-\left[\frac{2K}{I}\right]^2\right]^{1/2}\right]. \tag{9}$$

The break of stability of the stationary states is connected with the idea of cw switching proposed by Jensen [1]. However, the nonlinear switching itself is a much more complicated process which basically involved unstable states above the critical point. Nevertheless, in the framework of the model for the cw switching, exact analytical solutions may be found because the model is integrable.

The analysis briefly presented above may be compared with results given by the constant-width-pulse approach elaborated in Refs. [34,41,42] to analyze the pulse switching. The key point of that approach is to assume that pulse switching in the model (1) is realized through the approximate ansatz

$$u_1=\frac{\eta\sin\theta e^{i\phi_1}}{\cosh(\eta t)},\quad u_2=\frac{\eta\cos\theta e^{i\phi_2}}{\cosh(\eta t)}, \tag{10}$$

where the parameter η is constant, and two variational parameters are the effective angle θ, describing a relative difference of the pulse amplitudes in two optical modes, and $\phi=\phi_1-\phi_2$, the relative pulse phase, which are assumed to vary with ξ. The pulses (10) used in the variational approach [34,41,42] result in a system of ODE's for θ and ϕ which may be reduced to exactly the same as those given in Eqs. (6) and (7), provided $I=\frac{2}{3}\eta^2$. This simple observation means that the approach used in Refs. [34,41,42] formally coincides with the case of the cw switching, and this is why it does no allow us to obtain a deeper insight into the physics of pulse switching.

III. VARIATIONAL APPROACH AND PROPER TRIAL FUNCTIONS

The Lagrangian density $\mathcal{L}$ of (1) is given by

$$\mathcal{L}=\frac{i}{2}\left[u_1^*\frac{\partial u_1}{\partial\xi}+u_2^*\frac{\partial u_2}{\partial\xi}\right]-\frac{1}{4}\left[\left|\frac{\partial u_1}{\partial\tau}\right|^2+\left|\frac{\partial u_2}{\partial\tau}\right|^2-|u_1|^4-|u_2|^4\right]+Ku_1u_2^*+\text{c.c.}, \tag{11}$$

where c.c. stands for the complex conjugation.

The idea of the variational approach consists of inserting appropriate trial functions with free parameters into (11), performing the integration with respect to τ to find the average Lagrangian $L=\int_{-\infty}^{\infty}\mathcal{L}\,d\tau$, and varying it

with respect to the free parameters. Eventually, one ends up with the Euler-Lagrangian equations for those parameters that describe the evolution of the pulses (for details see, e.g., [15,16,34]).

As already mentioned, in using the variational approach the critical point is the proper choice of the trial functions because they should reflect, at least approximately, how the pulses evolve during the coupling process. In this respect it is of particular interest to assess the evolution of the pulse shape, the chirp, and the pulse width.

In order to do this we have launched numerically a fundamental soliton with the input peak power $|u_1(0,0)|^2=6$ into channel 1, which is a representative value because the BPM critical peak power is 6.592. Because we are interested in half-beat-length couplers ($\xi=\pi/2$) it suffices to concentrate slightly longer propagation distances. In Fig. 1 a comparison of the pulse shape provided by the BPM calculations is performed with proper sech functions for different propagation distances. It turns out that the sech shape is very well conserved, at least up to the half-beat length. As already stated, the chirp of the pulse is the crucial physical parameter that determines whether the pulse broadens (negative chirp), is compressed (positive chirp), or propagates without changing the width (zero chirp). Usually, the chirp is defined as the negative derivative of the time-dependent phase leading to a time-dependent frequency. In order to introduce a chirp parameter, we have to fit the phase with a polynomial. We denote the phase of the pulse by $\Phi_{(\mathrm{BPM})}(\tau_i)$ and define a polynomial as

$$\tilde{\Phi}(\xi,\tau)=a(x9)+b(\xi)\tau+q_{(\mathrm{BPM})}(\xi)\tau^2 . \quad (12)$$

We determine the parameters, a, b, and $q_{(\mathrm{BPM})}$ by sampling the pulse at discrete points τ_i and requiring

$$\left[\sum_{\tau_i}|u(\tau_i)|^2|\Phi_{(\mathrm{BPM})}(\tau_i)-\tilde{\Phi}(\tau_i;a,b,q)|^2\right]\rightarrow\min . \quad (13)$$

The parameter $q_{(\mathrm{BPM})}$ is then called the chirp parameter. Note that a positive value of the chirp parameter is equivalent to a negative (down) chirp. From Eq. (13) it is evident that the central part of the pulse provides the major contribution to the averaged chirp parameter. In Fig. 2 the evolution of the chirp parameter is plotted both for the bar and cross channels as a function of the propagation distance. It is interesting that the tendency in both channels is similar. After the coupling process has started the chirp increases and is negative. That behavior should ultimately lead to a pulse broadening in both channels, regardless of the fact that in the bar channel the amplitude decreases whereas it increases in the cross channel. Eventually, we investigated the behavior of the pulse width. To this end we defined the BPM pulse width $\eta^{-1}_{(\mathrm{BPM})}$ as

$$\frac{1}{\eta^2_{(\mathrm{BPM})}(\xi)}=\frac{12}{\pi^2}\frac{\int_{-\infty}^{\infty}\tau^2|u_\nu(\xi,\tau)|^2d\tau}{\int_{-\infty}^{\infty}|u_\nu(\xi,\tau)|^2d\tau}, \quad \nu=1,2 . \quad (14)$$

The results are shown in Fig. 3. As anticipated the width increases in both channels due to the negative chirp acquired in the course of the coupling process.

In estimating the results depicted in Figs. 1–3, we can draw the conclusion that the trial function may be sech shaped, and we may assume a common ξ-dependent width as well as chirp for both channels. Obviously, the two latter assumptions represent a fairly rough approximation, but they guarantee that all integrations in the Lagrangian defined through its density (11) can be performed analytically. Because one argument in favor of the variational approach is its simplicity, one should avoid complicating it by including numerical integration procedures. Furthermore, it is obvious that the trial functions used in previous papers ([34] use the constant width and zero chirp, [36] a width inversely proportional to the amplitude and zero chirp, and [37] a common, variable width, but zero chirp) do not properly reflect the

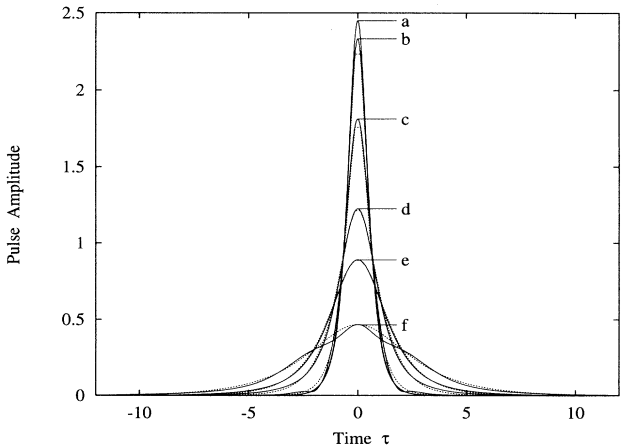

FIG. 1. Evolution of the pulse shape in channel 1; input peak power $P_1=6$. Solid lines: BPM results. Dotted lines: most similar sech-shaped pulses. (a) $\xi=0$, (b) $\xi=0.1\pi$, (c) $\xi=0.25\pi$, (d) $\xi=0.4\pi$, (e) $\xi=0.5\pi$, and (f) $\xi=0.75\pi$.

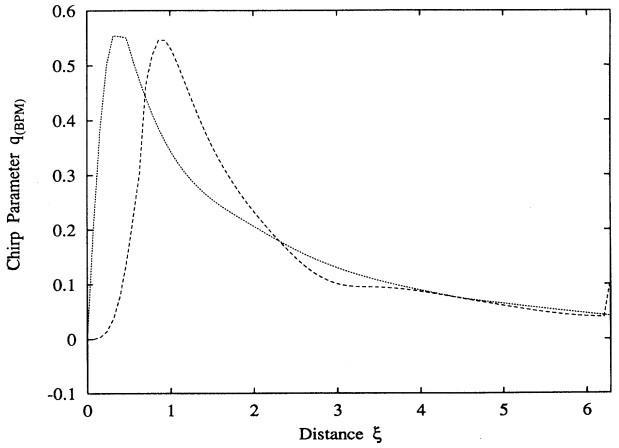

FIG. 2. Evolution of the chirp parameter [calculated by Eqs. (12) and (13)] of the pulses in both channels of the NLDC with input peak power $P_1=6$. Dashed line: bar channel. Dotted line: cross channel.

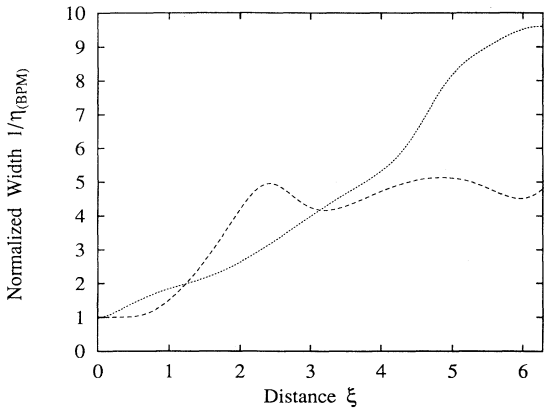

FIG. 3. Widths of the pulses in both channels [calculated by Eq. (14)] of the NLDC with input peak power $P=6$. Dashed line: bar channel. Dotted line: cross channel.

physics of the coupling process and the energy exchange between pulses belonging to the coupled channels. In conclusion, one should expect that such trial functions as

$$u_1(\xi,\tau)=a(\xi)\sqrt{\eta(\xi)}\,\mathrm{sech}[\eta(\xi)\tau]\cos[\Theta(\xi)] \times\exp\{i[\Phi(\xi)+\psi(\xi)+q(\xi)\tau^2]\}\ , \tag{15a}$$

$$u_2(\xi,\tau)=a(\xi)\sqrt{\eta(\xi)}\,\mathrm{sech}[\eta(\xi)\tau]\sin[\Theta(\xi)] \times\exp\{i[\Phi(\xi)-\psi(\xi)+q(\xi)\tau^2]\}\ , \tag{15b}$$

contain the principal effects taking place during the coupling process, and that they should lead to a reasonable improvement with respect to the characterization of the switching process. Note that the reliability of the trial functions chosen improves if one limits the coupler length, about one-half-beat length being the case we are interested in. The function $\Theta(\xi)$ describes the energy transfer between both channels similar to the case of cw switching, and $\Phi(\xi)$ is a common phase that plays no role in the dynamics of a directional coupler but comes into play if one investigates loop mirrors. $\psi(\xi)$ is twice the phase difference, and $\eta(\xi)$ is the inverse width. Similar trial functions have been used in analyzing nonlinear coupling in birefringent fibers [38–40].

IV. BASIC EQUATIONS OF THE VARIATIONAL APPROACH

In this section we derive the basis system of ODE's that governs the evolution of the pulse parameters during the coupling process.

Inserting the trial functions (15a) and (15b) into the Lagrangian density $\mathcal{L}$ (2) and integrating with respect to τ, we obtain the time-averaged Lagrangian L:

$$L=2Ka^2\cos(2\psi)\sin(2\Theta) -2a^2\cos(2\Theta)\frac{d\psi}{d\xi}-\tfrac{1}{3}a^4\eta\sin^2(2\Theta) +\tfrac{2}{3}a^4\eta-\tfrac{1}{3}a^2\eta^2-2a^2\frac{d\Phi}{d\xi}-\frac{1}{6}\frac{a^2\pi^2}{\eta^2}\left[\frac{dq}{d\xi}+2q^4\right]\ . \tag{16}$$

The variation of (16) with respect to all ξ-dependent parameters leads to a conserved quantity such as

$$\frac{da^2}{d\xi}=0 \tag{17a}$$

and Euler-Lagrangian equations for the parameters that remain:

$$\frac{d\Theta}{d\xi}=-K\sin(2\psi)\ , \tag{17b}$$

$$\sin(2\Theta)\frac{d\psi}{d\xi}=\frac{a^2}{3}\eta\sin(2\Theta)\cos(2\Theta) -K\cos(2\psi)\cos(2\Theta)\ , \tag{17c}$$

$$\frac{d\eta}{d\xi}=-2q\eta\ , \tag{17d}$$

$$\frac{dq}{d\xi}=-2q^2+\frac{2}{\pi^2}\{\eta^4-a^2\eta^3[1-\tfrac{1}{2}\sin^2(2\Theta)]\}\ . \tag{17e}$$

Note that Eqs. (17d) and (17e) reflect the mutual interplay between the width and chirp of the pulses. From the point of view of Hamiltonian mechanics, Eqs. (17b)–(17e) are the Hamiltonian equations of a two-degree-of-freedom model, where the phase difference and amplitude, determined by $\Theta(\xi)$, as well as the width and chirp, respectively, are conjugated variables.

The Hamiltonian of the system (17b)–(17e) is now written as

$$H=-2Ka^2\cos(2\psi)\sin(2\Theta)+\tfrac{1}{3}a^4\eta\sin^2(2\Theta) -\tfrac{2}{3}a^4\eta+\tfrac{1}{3}a^2\eta^2+\frac{\pi^2}{3}\frac{a^2}{\eta^2}q^2\ , \tag{18}$$

which represents another conserved quantity and which may be used to reduce the system to three coupled ODE's.

If $\eta=$const and $q=0$, we end up with the Paré-Florjanzcyk model [34] being a one-degree-of-freedom model, which allows us to adopt a quasiparticle picture where the remaining equations can be integrated analytically. Although the trial functions (15a) and (15b) have been used in [41,42], the authors have set the chirp to zero and assumed the width to be constant. Consequently, some terms are missing in the averaged Lagrangian, and the Eqs. (17d) and (17e) do not appear. Hence they are left with Paré-Florjanzcyk results.

Note that the ODE's (17b)–(17e) may be used to describe both power- and phase-controlled switching. The only difference consists of the different initial conditions. Furthermore, even effects such as symmetry breaking for symmetric or antisymmetric input pulses fed into both channels can be studied.

Obviously, the variational approach fails to predict the bifurcation picture of the antisymmetric solution, because both the antisymmetric solution and the asymmetric one branching off at the bifurcation points are unstable [33]. Hence the approach introduced here should be reliable if one studies switching processes in about one-half-beat length couplers.

V. POWER-CONTROLLED PULSE SWITCHING

In what follows we are going to solve system (17) for the case of power-controlled switching, which means that only one channel, say channel 1, is excited (one-channel input). Similarly, we solve Eq. (1) by a standard BPM procedure (see, e.g., [24]). We compare both the transmission characteristics that represent an integral quantity and the evolution of the pulse parameters provided by both procedures. Furthermore, besides the usual soliton input we used properly tailored Gaussian pulses as input and, showed that the behavior is similar and that even those pulses behave as stable objects in the course of the coupling process as mentioned above [35,37]. We concentrate first the soliton input

$$u_1(0,\tau)=a\sqrt{\eta(0)}\,\mathrm{sech}[\eta(0)\tau]\ , \tag{19}$$

where $a=\sqrt{\eta(0)}$.

First the energy transmission characteristics (switching curve) have been calculated. In Fig. 4 the straight-through transmission at the half-beat length $L_c=\pi/2$,

$$T=\frac{\int_{-\infty}^{\infty}|u_1(L_c,\tau)|^2 d\tau}{\int_{-\infty}^{\infty}|u_1(0,\tau)|^2 d\tau}\ , \tag{20}$$

is plotted as a function of the input peak power $P_1=|u_1(0,)|^2$. As usual, we define the critical switching power by requiring that $T=0.5$. It is evident that our model shows an excellent agreement with the numerical results (the BPM critical power is 6.592, and the critical power in our model is 6.775; the difference is 3% only). Moreover, the slope of the transmission curve is very similar to that provided by the BPM, and the respective shapes coincide for high input peak powers (see, for comparison, the large deviations that are provided by the constant width model). It is not surprising that the variational approach yields reasonable results for the integral quantity when using a proper trial function, but the question remains whether the pulse evolution is described adequately. To this end we study the evolution of the pulse parameters both by BPM and by our model for $P_1=4$, 6, and 8, representing input peak powers well below, close to, and well above the critical power, respectively. We show simultaneously the propagation of the pulses in both channels obtained from BPM calculations and the evolution of the peak amplitudes, the widths, and the chirp parameters, respectively, provided by both approaches. Width and peak powers are normalized with initial values for $\xi=0$. Furthermore, it turns out to be convenient to introduce an averaged width $1/\eta_{\mathrm{av}}$,

$$\frac{1}{\eta_{\mathrm{av}}^2(\xi)}=\frac{12}{\pi^2}\frac{\int_{-\infty}^{\infty}\tau^2(|u_1(\xi,\tau)|^2+|u_2(\xi,\tau)|^2)d\tau}{\int_{-\infty}^{\infty}(|u_1(\xi,\tau)|^2+|u_2(\xi,\tau)|^2)d\tau}\ . \tag{21}$$

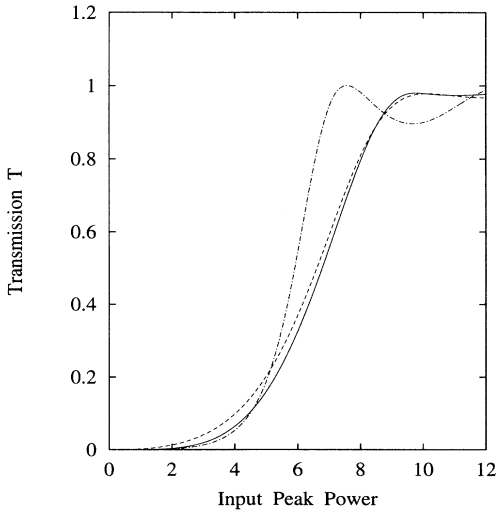

FIG. 4. Straight-through transmission (energy in the bar channel) of a one-half-beat-length NLDC as a function of the input peak power for soliton (sech-shaped) input pulse. Solid line: our model. Dashed line: BPM results. Dotted line: results given by the constant width model [33].

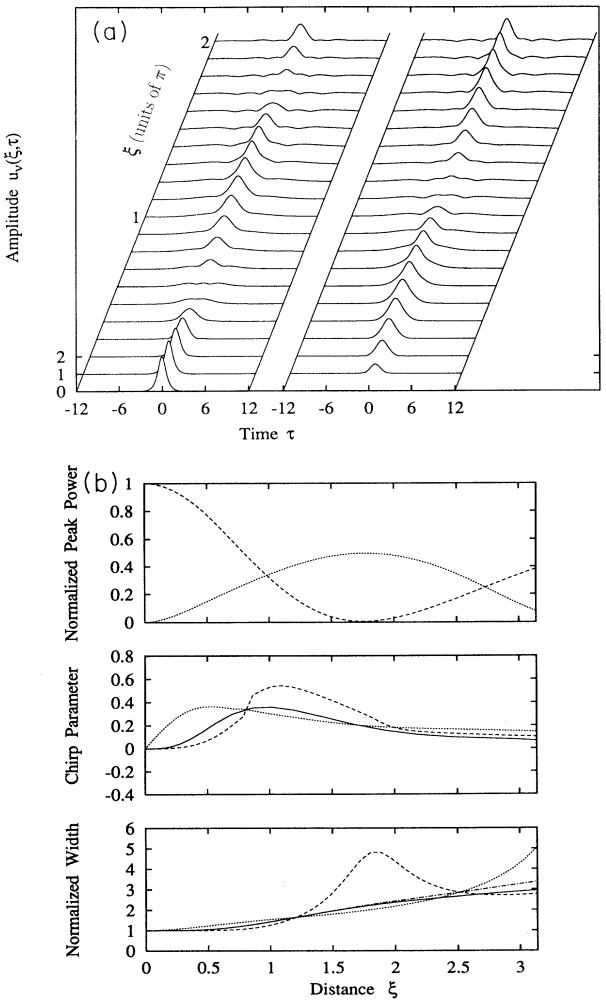

FIG. 5. (a) Evolution of the pulse in both channels of the NLDC for the input peak power $P_1=4$ (BPM). (b) Normalized peak power, chirp parameter, and normalized width, respectively, for $P_1=4$. Dashed and dotted lines: BPM results for bar and cross channel, respectively. Solid lines: our model. Dashed-dotted line: averaged width [calculated by Eq. (13)].

In Figs. 5–7 our results are plotted. The first conclusion is that in the whole region of powers, even over large propagation distances, neither pulse breakup nor the creation of new soliton states can be observed. Minor deviations from the sech shape can be identified for propagation distances that exceed the beat length ($\xi=\pi$). Second, it turns out that both the evolution of the widths and the chirps is qualitatively well described by the model, at least for a few half-beat lengths. In particular, if one takes into account that the differences with respect to width occur only at those propagation distances where the amplitude is almost zero, the agreement is even better. This is reflected by the behavior of the averaged width that practically coincides with the width calculated by using our model. In conclusion, there is surprisingly good quantitative agreement in the evolution of the pulse parameters between the numerical and variational approaches. This provides further evidence that the trial functions used are properly chosen, and that the variational approach may be used in modeling the nonlinear coupling in fiber couplers, at least as far as the one-channel input and half-beat length couplers are concerned.

Since the famous work of Anderson [15] it has been appreciated that Gaussian pulses with a definite relation between amplitude and width behave similarly to solitons. It has been shown that this holds true even for nonlinear coupling [35,37,40]. If one assumes trial functions similar to those in (15) and replaces only the sech function by a Gaussian, one ends up with the same kind of ODE's (17) where only minor differences concerning the coefficients arise. We have performed the BPM calculations as well as the solution for the ODE's. It shall suffice to present only the transmission characteristic (see Fig.

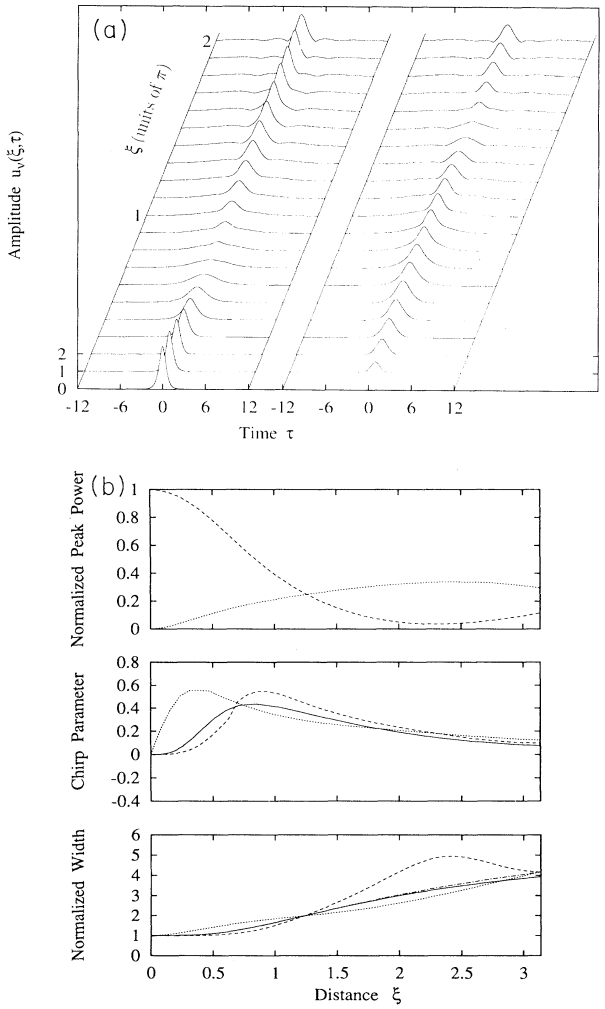

FIG. 6. (a) Evolution of the pulse in both channels of the NLDC for the input peak power $P_1=6$ (BPM). (b) Normalized peak power, chirp parameter, and normalized width, respectively, for $P_1=6$. Dashed and dotted lines: BPM results for bar and cross channels, respectively. Solid lines: our model. Dashed-dotted line: averaged width [calculated by Eq. (21)].

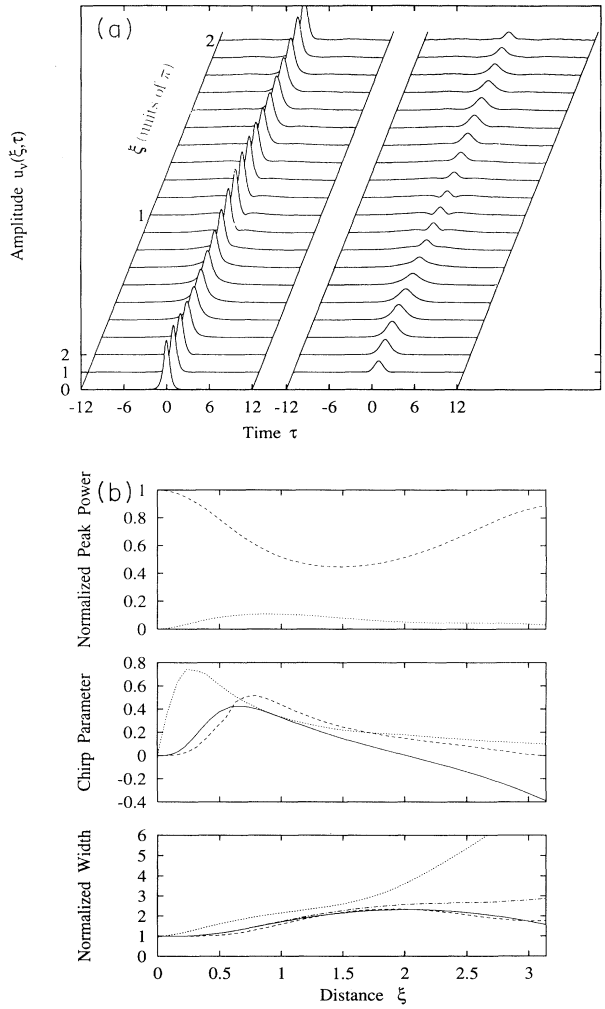

FIG. 7. (a) Evolution of the pulse in both channels of the NLDC for the input peak power $P_1=8$ (BPM). (b) Normalized peak power, chirp parameter, and normalized width, respectively, for $P_1=8$. Dashed and dotted lines: BPM results for bar and cross channels, respectively. Solid lines: our model. Dashed-dotted line: averaged width [calculated by Eq. (21)].

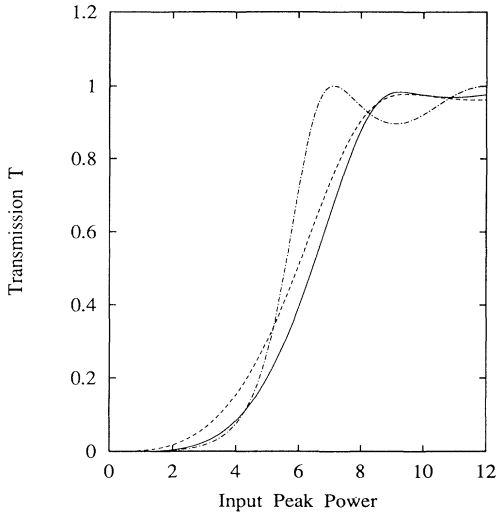

FIG. 8. Straight-through transmission (energy in the bar channel) of a one-half-beat-length NLDC as a function of the input peak power for Gaussian-shaped input pulse. Solid line: our model. Dashed line: BPM results. Dotted line: results given by the constant width model [33].

8). In comparing Figs. 8 and 4 it can clearly be recognized that the agreement between BPM and variational approaches worsens. This can be attributed mainly to the creation of small radiative waves that split off from the Gaussian, where the pulse remaining evolves toward a soliton. Of course, leaky radiation is also observed for the sech-profile pulses, but this is much smaller than in the case of Gaussian pulses. This difference may be explained by an extra amount of the so-called transition radiation, which should be emitted to form a pulse profile close to the solitonic one for which nonlinearity is perfectly balanced by dispersion. Such an effect can be easily understood for a single NLS equation where the transition radiation is usually observed during the pulse transformation (e.g., from a Gaussian input shape) into a sech-type profile. Nevertheless, even for that case the variational approach yields qualitatively satisfying results.

VI. PHASE-CONTROLLED PULSE SWITCHING

Phase-controlled switching in nonlinear directional couplers represents an attractive alternative to power-controlled switching. This was underscored a decade ago by Wabnitz *et al.* [5] for the cw case, and later on also investigated numerically for solitons [25,43]. The key idea is that one prepares the system appropriately in tuning it close to an unstable state (input signal in channel 1 slightly beyond the critical power). Now a weak input signal fed into the second channel affects the output signal critically depending on its phase [5,25,26,43]. The advantage is that one may control the output by changing the character of a weak input which is attractive for all-optical operations. It is well known from the cw case that a zero phase difference routes the output to the bar channel, whereas by a phase difference π the cross channel is addressed. Unfortunately, the situation is more involved than for power-controlled switching. What one wants to achieve is switching curves that are steep in a certain phase interval, and on the other hand, an output that is insensitive to phase changes over large phase intervals. Another requirement consists of a large switching contrast. Hence one may define a figure of merit (FOM) for phase-controlled switching that should contain features such as steep slopes, wide flat regions, and large contrast. The two essential parameters that one should vary in order to optimize that FOM are the device length and input peak power, because it is not evident that the FOM is maximized just at the half-beat length used as a device length in [25,43]. The reason for that anticipation is that one drives the system with a weak in-phase signal slightly below the critical power where complete coupling occurs, but with a nonlinear coupling length that exceeds the half-beat length. Hence, concerning soliton switching, numerical methods are not very appealing because one has to make a huge number of runs to identify the optimum FOM. In this respect, the variational approach seems very attractive for this optimization task. In what follows we use system (17) in order to determine the optimal configuration. Then we compare the switching curve obtained by the variational approach with that provided by the BPM. Now the input looks like

$$u_1(0,\tau)=a\sqrt{\eta(0)}\,\mathrm{sech}[\eta(0)\tau]\cos[\Theta(0)]\exp\{i[\psi(0)]\}\ , \tag{22}$$

$$u_2(0,\tau)=a\sqrt{\eta(0)}\,\mathrm{sech}[\eta(0)\tau]\sin[\Theta(0)]\exp\{-i[\psi(0)]\}\ ,$$

where $|\Theta(0)|\ll 1$ and $2\psi(0)$ is the phase difference. In Fig. 9 a contour plot of the FOM is shown where the maximum is situated in the center, and we have chosen $\sin[\Theta(0)]\approx 0.1$. It turns out that the optimum input peak power is $P_1=7.6$, which exceeds the critical power by 12% and that the optimum device length is $\xi=2.4$ as compared to the half-beat length $\xi=\pi/2$. The resulting switching curves, obtained from BPM and system (9), re-

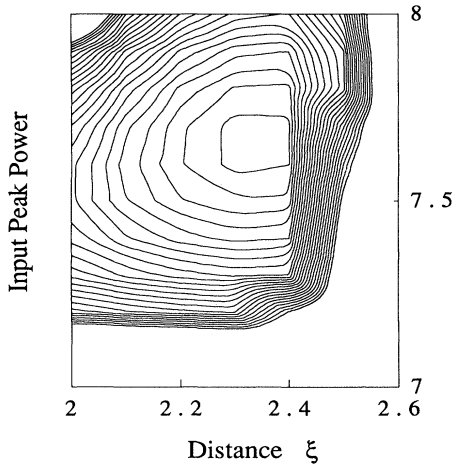

FIG. 9. Contour plot of the figure of merit as a function of the device length and the input peak power.

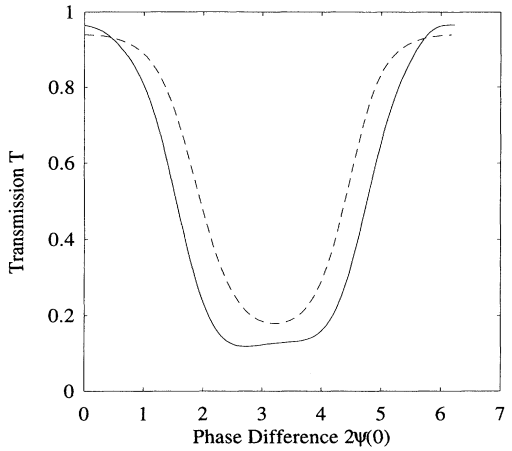

FIG. 10. Switching characteristics [transmission as a function of the initial phase difference $2\psi(0)$] for phase-controlled switching with input peak power $P_1=7.6$. Solid lines: our model. Dashed lines: BPM results.

spectively, are plotted in Fig. 10. Although the agreement is reasonable it can be improved further if one takes into account that the BPM critical power is a few percent less than that of our model (see Fig. 4). For example, if we use the peak power $P_1=7.2$ for the BPM calculations and $P_1=7.6$ for our model, we arrive at very similar results for the switching curves of Fig. 10.

We may conclude that the variational approach has its particular merits in describing phase-controlled switching because it is much more convenient for optimizing the input peak power and device length than the BPM.

VII. CONCLUSIONS

We have shown that a variational approach fits well to the description of the pulse dynamics in one-half-beat length nonlinear directional couplers, provided that suitable trial functions are identified. The key point is that one takes into account the inherent correlation between the pulse width and chirp. Concerning power-controlled switching (one-channel input) an excellent agreement between our results and numerically obtained switching curves could be identified. Moreover, even the essential parameters that characterize the pulse (amplitude, width, and chirp) have been shown to coincide fairly well. Furthermore, it turns out that the variational approach represents a useful tool in optimizing the configuration for phase-controlled switching conveniently. The resulting switching curves are in very good agreement with the BPM results if one takes into account a minor correction of the input peak power.

ACKNOWLEDGMENTS

Some authors (I.U., R.M., and F.L.) acknowledge the financial support of the Deutsche Forschungsgemeinschaft, Bonn, Germany, provided in the framework of the Sonderforschungsbereich 196. The work of Y.K. was partially supported by the Australian Photonics Cooperative Research Centre. I.U. was partly supported by the Bulgarian Foundation for Scientific Investigation, Contract No. F-49.

[1] S. M. Jensen, IEEE J. Quantum Electron. **QE-18**, 1580 (1982). Jensen defines a coherent coupler as a device which "··· utilizes the coherent interaction of two optical guides placed in close proximity. Because of the evanescent field overlap, these waveguides periodically exchange power."

[2] A. A. Maier, Kvant. Electron. (Moscow) **9**, 2296 (1982) [Sov. J. Quantum. Electron. **12**, 1490 (1982)].

[3] M. Romagnoli, S. Trillo, and S. Wabnitz, Opt. Quantum Electron. **24**, S1237 (1992).

[4] S. Trillo and S. Wabnitz, *Anisotropic and Nonlinear Optical Waveguides,* edited by C. S. Someda and G. Stegeman, (Elsevier, Amsterdam, 1992), p. 185.

[5] S. Wabnitz, E. M. Wright, C. T. Seaton, and G. I. Stegeman, Appl. Phys. Lett. **53**, 837 (1986).

[6] S. Trillo, S. Wabnitz, R. H. Stolen, G. Assanto, C. T. Seaton, and G. I. Stegeman, Appl. Phys. Lett. **49**, 1224 (1986).

[7] D. D. Gusovski, E. M. Dianov, A. A. Maier, V. B. Neustreuev, E. I. Shklovskii, and A. Shcherbakov, Kvant. Electron. (Moscow) **14**, 1144 (1987) [Sov. J. Quantum. Electron. **17**, 724 (1987)].

[8] A. A. Maier, Yu. N. Serdyuchenko, K. Yu. Sitarskii, M. Ya. Shchelev, and I. A. Shcherbakov, Kvant. Electron. (Moscow) **14**, 1157 (1987) [Sov. J. Quantum. Electron. **17**, 735 (1987)].

[9] S. R. Friberg, Y. Siberberg, M. K. Oliver, M. J. Andrejko, M. A. Saifi, and P. W. Smith, Appl. Phys. Lett. **51**, 1135 (1987).

[10] S. R. Friberg, A. M. Weiner, Y. Silberberg, B. G. Sfez, and P. S. Smith, Opt. Lett. **13**, 904 (1988).

[11] S. Trillo, S. Wabnitz, N. Finlayson, W. C. Banyai, C. T. Seaton, G. I. Stegeman, and R. H. Stolen, Appl. Phys. Lett. **53**, 837 (1988).

[12] S. Trillo, S. Wabnitz, W. C. Banyai, N. Finlayson, C. T. Seaton, G. I. Stegeman, and R. H. Stolen, IEEE J. Quantum Electron. **25**, 104 (1989).

[13] A. Hasegawa, *Optical Solitons in Fibers* (Springer, Berlin, 1989).

[14] G. P. Agrawal, *Nonlinear Fiber Optics* (Academic, New York, 1989).

[15] D. Anderson, Phys. Rev. A **27**, 3135 (1983).

[16] D. Anserson, M. Lisak, and T. Reichel, J. Opt. Soc. Am. B **5**, 207 (1988).

[17] N. J. Doran and D. Wood, J. Opt. Soc. Am. B **4**, 1843 (1987).

[18] K. J. Blow, N. J. Doran, and B. K. Nayar, Opt. Lett. **14**, 754 (1989).

[19] K. J. Blow, N. J. Doran, and D. Wood, Opt. Lett. **12**, 202 (1987).

[20] S. Trillo, S. Wabnitz, E. M. Wright, and G. I. Stegeman, Opt. Lett. **13**, 672 (1988).

[21] S. Trillo, S. Wabnitz, E. M. Wright, and G. I. Stegeman, Opt. Commun. **70**, 166 (1989).
[22] V. E. Zakharov and A. B. Shabat, Zh. Eksp. Teor. Fiz. **61**, 118 (1971) [Sov. Phys. JETP. **34**, 62 (1972)].
[23] S. V. Manakov, Zh. Eksp. Teor. Fiz. **65**, 505 (1973) [Sov. Phys. JETP. **38**, 248 (1974)].
[24] D. Yevick and B. Hermansson, Opt. Commun. **47**, 101 (1983); T. R. Taha and M. J. Ablowitz, J. Comput. Phys. **55**, 203 (1984).
[25] J. Soto-Crespo and E. M. Wright, J. Appl. Phys. **70**, 7240 (1991).
[26] C. Schmidt-Hattenberger, R. Muschall, F. Lederer, and U. Trutschel, J. Opt. Soc. Am. B **10**, 592 (1993).
[27] Yu. S. Kivshar, Opt. Lett. **18**, 1147 (1993).
[28] R. Muschall, C. Schmidt-Hattenberger, and F. Lederer, Opt. Lett. **19**, 323 (1994).
[29] F. Kh. Abdullaev, R. M. Abrarov, and S. A. Darmanyan, Opt. Lett. **14**, 131 (1989).
[30] Yu. S. Kivshar and B. A. Malomed, Opt. Lett. **14**, 1365 (1989).
[31] N. Akhmediev and A. Ankiewicz, Phys. Rev. Lett. **70**, 2395 (1993).
[32] A. Ankiewicz, N. Akhmediev, G. D. Peng, and P. L. Chu, Opt. Commun. **103**, 410 (1993).
[33] J. M. Soto-Crespo and N. Akhmediev, Phys. Rev. E **48**, 4710 (1993).
[34] C. Paré and M. Florjanzcyk, Phys. Rev. A **41**, 6287 (1990).
[35] E. Caglioti, S. Trillo, S. Wabnitz, B. Crosignani, and P. Di Porto, J. Opt. Soc. Am. B **7**, 374 (1990).
[36] Yu. S. Kivshar, Opt. Lett. **18**, 7 (1993).
[37] F. Lederer and I. M. Uzunov, in *Nonlinear Guided-Wave Phenomena,* Technical Digest Vol. 15 (Washington, D. C., 1993), pp. 108–111.
[38] T. Ueda and W. L. Kath, Phys. Rev. A **42**, 563 (1990).
[39] D. J. Muraki and W. L. Kath, Physica D **48**, 53 (1991).
[40] D. J. Kaup, B. A. Malomed, and R. S. Tasgal, Phys. Rev. E **48**, 3049 (1993).
[41] P. L. Chu, G. D. Peng, and B. A. Malomed, Opt. Lett. **18**, 328 (1993).
[42] P. L. Chu, B. A. Malomed, and G. D. Peng, J. Opt. Soc. Am. B **8**, 1379 (1993).
[43] S. Trillo and S. Wabnitz, Opt. Lett. **16**, 1 (1991).